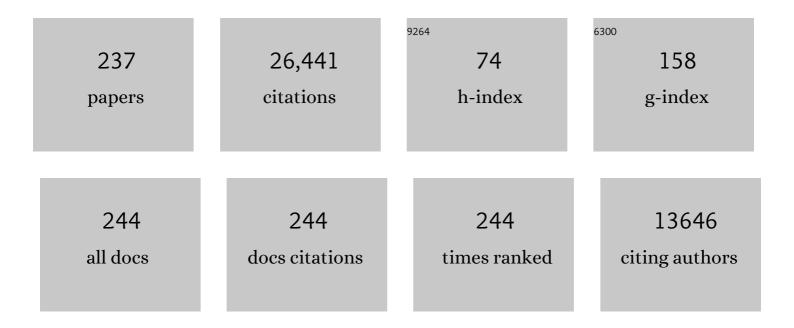
## Frederic Baret

List of Publications by Year in descending order

Source: https://exaly.com/author-pdf/6059310/publications.pdf Version: 2024-02-01



FDEDEDIC RADET

#	Article	IF	CITATIONS
1	PROSPECT: A model of leaf optical properties spectra. Remote Sensing of Environment, 1990, 34, 75-91.	11.0	1,841
2	Optimization of soil-adjusted vegetation indices. Remote Sensing of Environment, 1996, 55, 95-107.	11.0	1,801
3	Potentials and limits of vegetation indices for LAI and APAR assessment. Remote Sensing of Environment, 1991, 35, 161-173.	11.0	1,514
4	PROSPECT+SAIL models: A review of use for vegetation characterization. Remote Sensing of Environment, 2009, 113, S56-S66.	11.0	1,178
5	Review of methods for in situ leaf area index determination. Agricultural and Forest Meteorology, 2004, 121, 19-35.	4.8	1,164
6	Review of methods for in situ leaf area index (LAI) determination. Agricultural and Forest Meteorology, 2004, 121, 37-53.	4.8	793
7	LAI, fAPAR and fCover CYCLOPES global products derived from VEGETATION. Remote Sensing of Environment, 2007, 110, 275-286.	11.0	734
8	Retrieval of canopy biophysical variables from bidirectional reflectance. Remote Sensing of Environment, 2003, 84, 1-15.	11.0	545
9	GEOV1: LAI and FAPAR essential climate variables and FCOVER global time series capitalizing over existing products. Part1: Principles of development and production. Remote Sensing of Environment, 2013, 137, 299-309.	11.0	488
10	An Overview of Global Leaf Area Index (LAI): Methods, Products, Validation, and Applications. Reviews of Geophysics, 2019, 57, 739-799.	23.0	396
11	Hyperspectral remote sensing of foliar nitrogen content. Proceedings of the National Academy of Sciences of the United States of America, 2013, 110, E185-92.	7.1	389
12	Relating soil surface moisture to reflectance. Remote Sensing of Environment, 2002, 81, 238-246.	11.0	379
13	Assessment of Unmanned Aerial Vehicles Imagery for Quantitative Monitoring of Wheat Crop in Small Plots. Sensors, 2008, 8, 3557-3585.	3.8	377
14	Validation and intercomparison of global Leaf Area Index products derived from remote sensing data. Journal of Geophysical Research, 2008, 113, .	3.3	363
15	Extraction of vegetation biophysical parameters by inversion of the PROSPECT + SAIL models on sugar beet canopy reflectance data. Application to TM and AVIRIS sensors. Remote Sensing of Environment, 1995, 52, 163-172.	11.0	349
16	Validation of global moderate-resolution LAI products: a framework proposed within the CEOS land product validation subgroup. IEEE Transactions on Geoscience and Remote Sensing, 2006, 44, 1804-1817.	6.3	341
17	Investigation of a model inversion technique to estimate canopy biophysical variables from spectral and directional reflectance data. Agronomy for Sustainable Development, 2000, 20, 3-22.	0.8	337
18	Leaf optical properties with explicit description of its biochemical composition: Direct and inverse problems. Remote Sensing of Environment, 1996, 56, 104-117.	11.0	332

Frederic Baret

#	Article	IF	CITATIONS
19	Neural network estimation of LAI, fAPAR, fCover and LAI×Cab, from top of canopy MERIS reflectance data: Principles and validation. Remote Sensing of Environment, 2006, 105, 313-325.	11.0	331
20	LAI and fAPAR CYCLOPES global products derived from VEGETATION. Part 2: validation and comparison with MODIS collection 4 products. Remote Sensing of Environment, 2007, 110, 317-331.	11.0	313
21	Estimates of plant density of wheat crops at emergence from very low altitude UAV imagery. Remote Sensing of Environment, 2017, 198, 105-114.	11.0	312
22	Intercalibration of vegetation indices from different sensor systems. Remote Sensing of Environment, 2003, 88, 412-422.	11.0	306
23	GEOV1: LAI, FAPAR essential climate variables and FCOVER global time series capitalizing over existing products. Part 2: Validation and intercomparison with reference products. Remote Sensing of Environment, 2013, 137, 310-329.	11.0	297
24	A ratio vegetation index adjusted for soil brightness. International Journal of Remote Sensing, 1990, 11, 727-740.	2.9	258
25	High-Throughput Phenotyping of Plant Height: Comparing Unmanned Aerial Vehicles and Ground LiDAR Estimates. Frontiers in Plant Science, 2017, 8, 2002.	3.6	240
26	Modeling spectral and bidirectional soil reflectance. Remote Sensing of Environment, 1992, 41, 123-132.	11.0	239
27	Developments in the 'validation' of satellite sensor products for the study of the land surface. International Journal of Remote Sensing, 2000, 21, 3383-3390.	2.9	237
28	Estimation of soil clay and calcium carbonate using laboratory, field and airborne hyperspectral measurements. Remote Sensing of Environment, 2008, 112, 825-835.	11.0	235
29	Quantifying spatial heterogeneity at the landscape scale using variogram models. Remote Sensing of Environment, 2006, 103, 81-96.	11.0	206
30	The robustness of canopy gap fraction estimates from red and near-infrared reflectances: A comparison of approaches. Remote Sensing of Environment, 1995, 54, 141-151.	11.0	202
31	Estimation of leaf area and clumping indexes of crops with hemispherical photographs. Agricultural and Forest Meteorology, 2008, 148, 644-655.	4.8	200
32	Comparative analysis of three chemometric techniques for the spectroradiometric assessment of canopy chlorophyll content in winter wheat. Computers and Electronics in Agriculture, 2010, 73, 165-173.	7.7	199
33	Modeled analysis of the biophysical nature of spectral shifts and comparison with information content of broad bands. Remote Sensing of Environment, 1992, 41, 133-142.	11.0	195
34	Use of coupled canopy structure dynamic and radiative transfer models to estimate biophysical canopy characteristics. Remote Sensing of Environment, 2005, 95, 115-124.	11.0	195
35	Ear density estimation from high resolution RGB imagery using deep learning technique. Agricultural and Forest Meteorology, 2019, 264, 225-234.	4.8	190
36	Estimating light absorption by chlorophyll, leaf and canopy in a deciduous broadleaf forest using MODIS data and a radiative transfer model. Remote Sensing of Environment, 2005, 99, 357-371.	11.0	189

#	Article	IF	CITATIONS
37	Evaluation of the representativeness of networks of sites for the global validation and intercomparison of land biophysical products: proposition of the CEOS-BELMANIP. IEEE Transactions on Geoscience and Remote Sensing, 2006, 44, 1794-1803.	6.3	187
38	Quantification of plant stress using remote sensing observations and crop models: the case of nitrogen management. Journal of Experimental Botany, 2006, 58, 869-880.	4.8	187
39	Evaluation of Canopy Biophysical Variable Retrieval Performances from the Accumulation of Large Swath Satellite Data. Remote Sensing of Environment, 1999, 70, 293-306.	11.0	168
40	Fractional vegetation cover estimation algorithm for Chinese GF-1 wide field view data. Remote Sensing of Environment, 2016, 177, 184-191.	11.0	167
41	Remote sensing and crop production models: present trends. ISPRS Journal of Photogrammetry and Remote Sensing, 1992, 47, 145-161.	11.1	159
42	A comparison of methods for smoothing and gap filling time series of remote sensing observations – application to MODIS LAI products. Biogeosciences, 2013, 10, 4055-4071.	3.3	157
43	Intercomparison and sensitivity analysis of Leaf Area Index retrievals from LAI-2000, AccuPAR, and digital hemispherical photography over croplands. Agricultural and Forest Meteorology, 2008, 148, 1193-1209.	4.8	156
44	Validation of coarse spatial resolution LAI and FAPAR time series over cropland in southwest France. Remote Sensing of Environment, 2013, 139, 216-230.	11.0	155
45	Green area index from an unmanned aerial system over wheat and rapeseed crops. Remote Sensing of Environment, 2014, 152, 654-664.	11.0	151
46	Influence of landscape spatial heterogeneity on the non-linear estimation of leaf area index from moderate spatial resolution remote sensing data. Remote Sensing of Environment, 2006, 105, 286-298.	11.0	149
47	Characterization and intercomparison of global moderate resolution leaf area index (LAI) products: Analysis of climatologies and theoretical uncertainties. Journal of Geophysical Research G: Biogeosciences, 2013, 118, 529-548.	3.0	149
48	Estimating Canopy Characteristics from Remote Sensing Observations: Review of Methods and Associated Problems. , 2008, , 173-201.		144
49	Optimal modalities for radiative transfer-neural network estimation of canopy biophysical characteristics: Evaluation over an agricultural area with CHRIS/PROBA observations. Remote Sensing of Environment, 2011, 115, 415-426.	11.0	142
50	GAI estimates of row crops from downward looking digital photos taken perpendicular to rows at 57.5Ű zenith angle: Theoretical considerations based on 3D architecture models and application to wheat crops. Agricultural and Forest Meteorology, 2010, 150, 1393-1401.	4.8	137
51	Data Service Platform for Sentinel-2 Surface Reflectance and Value-Added Products: System Use and Examples. Remote Sensing, 2016, 8, 938.	4.0	132
52	Coupling canopy functioning and radiative transfer models for remote sensing data assimilation. Agricultural and Forest Meteorology, 2001, 108, 113-128.	4.8	129
53	Global Wheat Head Detection (GWHD) Dataset: A Large and Diverse Dataset of High-Resolution RGB-Labelled Images to Develop and Benchmark Wheat Head Detection Methods. Plant Phenomics, 2020, 2020, 3521852.	5.9	128
54	Performances of neural networks for deriving LAI estimates from existing CYCLOPES and MODIS products. Remote Sensing of Environment, 2008, 112, 2789-2803.	11.0	125

#	Article	IF	CITATIONS
55	Estimation of leaf water content and specific leaf weight from reflectance and transmittance measurements. Agronomy for Sustainable Development, 1997, 17, 455-464.	0.8	118
56	Vegetation water and dry matter contents estimated from top-of-the-atmosphere reflectance data: A simulation study. Remote Sensing of Environment, 1997, 61, 34-45.	11.0	115
57	Exploiting the centimeter resolution of UAV multispectral imagery to improve remote-sensing estimates of canopy structure and biochemistry in sugar beet crops. Remote Sensing of Environment, 2019, 231, 110898.	11.0	115
58	Albedo and LAI estimates from FORMOSAT-2 data for crop monitoring. Remote Sensing of Environment, 2009, 113, 716-729.	11.0	112
59	Simple and robust methods for remote sensing of canopy chlorophyll content: a comparative analysis of hyperspectral data for different types of vegetation. Plant, Cell and Environment, 2016, 39, 2609-2623.	5.7	109
60	Estimating leaf chlorophyll content in sugar beet canopies using millimeter- to centimeter-scale reflectance imagery. Remote Sensing of Environment, 2017, 198, 173-186.	11.0	108
61	Near Real-Time Vegetation Monitoring at Global Scale. IEEE Journal of Selected Topics in Applied Earth Observations and Remote Sensing, 2014, 7, 3473-3481.	4.9	106
62	A semi-automatic system for high throughput phenotyping wheat cultivars in-field conditions: description and first results. Functional Plant Biology, 2012, 39, 914.	2.1	104
63	What is cost-efficient phenotyping? Optimizing costs for different scenarios. Plant Science, 2019, 282, 14-22.	3.6	103
64	On spectral estimates of fresh leaf biochemistry. International Journal of Remote Sensing, 1998, 19, 1283-1297.	2.9	101
65	Vegetation baseline phenology from kilometric global LAI satellite products. Remote Sensing of Environment, 2016, 178, 1-14.	11.0	101
66	Evaluation of methods for soil surface moisture estimation from reflectance data. International Journal of Remote Sensing, 2003, 24, 2069-2083.	2.9	98
67	Crop residue estimation using multiband reflectance. Remote Sensing of Environment, 1997, 59, 530-536.	11.0	97
68	Use of spectral analogy to evaluate canopy reflectance sensitivity to leaf optical properties. Remote Sensing of Environment, 1994, 48, 253-260.	11.0	95
69	Retrieving wheat Green Area Index during the growing season from optical time series measurements based on neural network radiative transfer inversion. Remote Sensing of Environment, 2011, 115, 887-896.	11.0	94
70	Using 3D Point Clouds Derived from UAV RGB Imagery to Describe Vineyard 3D Macro-Structure. Remote Sensing, 2017, 9, 111.	4.0	94
71	Quality Assessment of PROBA-V LAI, fAPAR and fCOVER Collection 300 m Products of Copernicus Global Land Service. Remote Sensing, 2020, 12, 1017.	4.0	91
72	Assessing the biomass dynamics of Andean bofedal and totora high-protein wetland grasses from NOAA/AVHRR. Remote Sensing of Environment, 2003, 85, 516-529.	11.0	86

#	Article	IF	CITATIONS
73	Improving canopy variables estimation from remote sensing data by exploiting ancillary information. Case study on sugar beet canopies. Agronomy for Sustainable Development, 2002, 22, 205-215.	0.8	86
74	Lidar sheds new light on plant phenomics for plant breeding and management: Recent advances and future prospects. ISPRS Journal of Photogrammetry and Remote Sensing, 2021, 171, 202-223.	11.1	82
75	About the soil line concept in remote sensing. Advances in Space Research, 1993, 13, 281-284.	2.6	78
76	Effect of senescent leaves on NDVI-based estimates of fAPAR: Experimental and modelling evidences. International Journal of Remote Sensing, 2004, 25, 5415-5427.	2.9	78
77	A multisensor fusion approach to improve LAI time series. Remote Sensing of Environment, 2011, 115, 2460-2470.	11.0	75
78	Wheat leaf bidirectional reflectance measurements: Description and quantification of the volume, specular and hot-spot scattering features. Remote Sensing of Environment, 2012, 121, 26-35.	11.0	73
79	Crop biomass evaluation using radiometric measurements. Photogrammetria, 1989, 43, 241-256.	0.2	71
80	The CACAO Method for Smoothing, Gap Filling, and Characterizing Seasonal Anomalies in Satellite Time Series. IEEE Transactions on Geoscience and Remote Sensing, 2013, 51, 1963-1972.	6.3	70
81	A Generic Algorithm to Estimate LAI, FAPAR and FCOVER Variables from SPOT4_HRVIR and Landsat Sensors: Evaluation of the Consistency and Comparison with Ground Measurements. Remote Sensing, 2015, 7, 15494-15516.	4.0	70
82	Evaluation of an improved version of SAIL model for simulating bidirectional reflectance of sugar beet canopies. Remote Sensing of Environment, 1997, 60, 247-257.	11.0	69
83	Characterization of seasonal variation of forest canopy in a temperate deciduous broadleaf forest, using daily MODIS data. Remote Sensing of Environment, 2006, 105, 189-203.	11.0	69
84	Crop specific green area index retrieval from MODIS data at regional scale by controlling pixel-target adequacy. Remote Sensing of Environment, 2011, 115, 2686-2701.	11.0	69
85	Modeling maize canopy 3D architecture. Ecological Modelling, 1999, 122, 25-43.	2.5	68
86	Stochastic Modeling of Radiation Regime in Discontinuous Vegetation Canopies. Remote Sensing of Environment, 2000, 74, 125-144.	11.0	68
87	Multitemporal-patch ensemble inversion of coupled surface–atmosphere radiative transfer models for land surface characterization. Remote Sensing of Environment, 2008, 112, 851-861.	11.0	68
88	Validation of neural net techniques to estimate canopy biophysical variables from remote sensing data. Agronomy for Sustainable Development, 2002, 22, 547-553.	0.8	65
89	Monitoring wheat canopies with a high spectral resolution radiometer. Remote Sensing of Environment, 1987, 22, 367-378.	11.0	64
90	Forcing a wheat crop model with LAI data to access agronomic variables: Evaluation of the impact of model and LAI uncertainties and comparison with an empirical approach. European Journal of Agronomy, 2012, 37, 1-10.	4.1	64

#	Article	IF	CITATIONS
91	MARMIT: A multilayer radiative transfer model of soil reflectance to estimate surface soil moisture content in the solar domain (400–2500‬nm). Remote Sensing of Environment, 2018, 217, 1-17.	11.0	64
92	Polarization of Light by Vegetation. , 1991, , 191-228.		61
93	ACT: A leaf BRDF model taking into account the azimuthal anisotropy of monocotyledonous leaf surface. Remote Sensing of Environment, 2014, 143, 112-121.	11.0	61
94	The MODIS (collection V006) BRDF/albedo product MCD43D: Temporal course evaluated over agricultural landscape. Remote Sensing of Environment, 2015, 170, 216-228.	11.0	60
95	Estimation of Wheat Plant Density at Early Stages Using High Resolution Imagery. Frontiers in Plant Science, 2017, 8, 739.	3.6	60
96	Global Wheat Head Detection 2021: An Improved Dataset for Benchmarking Wheat Head Detection Methods. Plant Phenomics, 2021, 2021, 9846158.	5.9	60
97	Review Article Procedures for the description of agricultural crops and soils in optical and microwave remote sensing studies. International Journal of Remote Sensing, 1987, 8, 427-439.	2.9	57
98	Multivariate quantification of landscape spatial heterogeneity using variogram models. Remote Sensing of Environment, 2008, 112, 216-230.	11.0	57
99	Estimating wheat green area index from ground-based LiDAR measurement using a 3D canopy structure model. Agricultural and Forest Meteorology, 2017, 247, 12-20.	4.8	57
100	Enhanced Automated Canopy Characterization from Hyperspectral Data by a Novel Two Step Radiative Transfer Model Inversion Approach. Remote Sensing, 2009, 1, 1139-1170.	4.0	56
101	On Line Validation Exercise (OLIVE): A Web Based Service for the Validation of Medium Resolution Land Products. Application to FAPAR Products. Remote Sensing, 2014, 6, 4190-4216.	4.0	56
102	Land Cover and Crop Type Classification along the Season Based on Biophysical Variables Retrieved from Multi-Sensor High-Resolution Time Series. Remote Sensing, 2015, 7, 10400-10424.	4.0	54
103	Complementarity of middle-infrared with visible and near-infrared reflectance for monitoring wheat canopies. Remote Sensing of Environment, 1988, 26, 213-225.	11.0	49
104	A 30+ Year AVHRR Land Surface Reflectance Climate Data Record and Its Application to Wheat Yield Monitoring. Remote Sensing, 2017, 9, 296.	4.0	49
105	Leaf-rolling in maize crops: from leaf scoring to canopy-level measurements for phenotyping. Journal of Experimental Botany, 2018, 69, 2705-2716.	4.8	49
106	Training a neural network with a canopy reflectance model to estimate crop leaf area index. International Journal of Remote Sensing, 2003, 24, 4891-4905.	2.9	48
107	Evaluation of Agreement Between Space Remote Sensing SPOT-VEGETATION fAPAR Time Series. IEEE Transactions on Geoscience and Remote Sensing, 2013, 51, 1951-1962.	6.3	47
108	Estimation of Nitrogen Nutrition Status in Winter Wheat From Unmanned Aerial Vehicle Based Multi-Angular Multispectral Imagery. Frontiers in Plant Science, 2019, 10, 1601.	3.6	47

#	Article	IF	CITATIONS
109	The use of remotely sensed data in estimation of PAR use efficiency and biomass production of flooded rice. Remote Sensing of Environment, 1991, 38, 147-158.	11.0	45
110	Spectral estimates of the absorbed photosynthetically active radiation and light-use efficiency of a winter wheat crop subjected to nitrogen and water deficienciesâ€. International Journal of Remote Sensing, 1990, 11, 1797-1808.	2.9	44
111	Modeling directional brightness temperature over a maize canopy in row structure. IEEE Transactions on Geoscience and Remote Sensing, 2004, 42, 2290-2304.	6.3	44
112	Simultaneous determination of aerosol- and surface characteristics from top-of-atmosphere reflectance using MERIS on board of ENVISAT. Advances in Space Research, 2006, 37, 2172-2177.	2.6	44
113	Local Vegetation Trends in the Sahel of Mali and Senegal Using Long Time Series FAPAR Satellite Products and Field Measurement (1982–2010). Remote Sensing, 2014, 6, 2408-2434.	4.0	44
114	Radiation use efficiency of pearl millet in the Sahelian zone. Agricultural and Forest Meteorology, 1991, 56, 93-110.	4.8	42
115	A technique for determination of single leaf reflectance and transmittance in field studies. Remote Sensing of Environment, 1993, 43, 209-215.	11.0	40
116	Optimal geometric configuration and algorithms for LAI indirect estimates under row canopies: The case of vineyards. Agricultural and Forest Meteorology, 2009, 149, 1307-1316.	4.8	40
117	Suitability of modelled and remotely sensed essential climate variables for monitoring Euro-Mediterranean droughts. Geoscientific Model Development, 2014, 7, 931-946.	3.6	40
118	Estimation of leaf traits from reflectance measurements: comparison between methods based on vegetation indices and several versions of the PROSPECT model. Plant Methods, 2018, 14, 23.	4.3	40
119	Assimilating optical and radar data into the STICS crop model for wheat. Agronomy for Sustainable Development, 2003, 23, 297-303.	0.8	40
120	Sensitivity of gap fraction to maize architectural characteristics based on 4D model simulations. Agricultural and Forest Meteorology, 2007, 143, 217-229.	4.8	39
121	Remotely sensed green area index for winter wheat crop monitoring: 10-Year assessment at regional scale over a fragmented landscape. Agricultural and Forest Meteorology, 2012, 166-167, 156-168.	4.8	39
122	A High-Throughput Model-Assisted Method for Phenotyping Maize Green Leaf Area Index Dynamics Using Unmanned Aerial Vehicle Imagery. Frontiers in Plant Science, 2019, 10, 685.	3.6	39
123	Vineyard identification and description of spatial crop structure by per-field frequency analysis. International Journal of Remote Sensing, 2002, 23, 3311-3325.	2.9	36
124	Estimation of Plant and Canopy Architectural Traits Using the Digital Plant Phenotyping Platform. Plant Physiology, 2019, 181, 881-890.	4.8	36
125	A 3D peach canopy model used to evaluate the effect of tree architecture and density on photosynthesis at a range of scales. Ecological Modelling, 2000, 128, 197-209.	2.5	34
126	Slope correction for LAI estimation from gap fraction measurements. Agricultural and Forest Meteorology, 2008, 148, 1553-1562.	4.8	34

#	Article	IF	CITATIONS
127	Joint assimilation of eddy covariance flux measurements and FAPAR products over temperate forests within a processâ€oriented biosphere model. Journal of Geophysical Research G: Biogeosciences, 2015, 120, 1839-1857.	3.0	34
128	Exploring the spatial relationship between airborne-derived red and far-red sun-induced fluorescence and process-based GPP estimates in a forest ecosystem. Remote Sensing of Environment, 2019, 231, 111272.	11.0	34
129	Estimation à partir de mesures de réflectance spectrale du rayonnement photosynthétiquement actif absorbé par une culture de blé. Agronomy for Sustainable Development, 1989, 9, 885-895.	0.8	34
130	Hemispherical reflectance and albedo estimates from the accumulation of across-track sun-synchronous satellite data. Journal of Geophysical Research, 1999, 104, 22221-22232.	3.3	33
131	GEOCLIM: A global climatology of LAI, FAPAR, and FCOVER from VEGETATION observations for 1999–2010. Remote Sensing of Environment, 2015, 166, 126-137.	11.0	33
132	Estimates of Maize Plant Density from UAV RGB Images Using Faster-RCNN Detection Model: Impact of the Spatial Resolution. Plant Phenomics, 2021, 2021, 9824843.	5.9	32
133	Spatial and Temporal Variation of Light inside Peach Trees. Journal of the American Society for Horticultural Science, 1994, 119, 669-677.	1.0	32
134	Using First- and Second-Order Variograms for Characterizing Landscape Spatial Structures From Remote Sensing Imagery. IEEE Transactions on Geoscience and Remote Sensing, 2007, 45, 1823-1834.	6.3	31
135	Effect of thinning on LAI variance in heterogeneous forests. Forest Ecology and Management, 2008, 256, 890-899.	3.2	31
136	High-Throughput Measurements of Stem Characteristics to Estimate Ear Density and Above-Ground Biomass. Plant Phenomics, 2019, 2019, 4820305.	5.9	31
137	Soil surface infiltration capacity classification based on the bi-directional reflectance distribution function sampled by aerial photographs. The case of vineyards in a Mediterranean area. Catena, 2005, 62, 94-110.	5.0	30
138	An automatic method based on daily in situ images and deep learning to date wheat heading stage. Field Crops Research, 2020, 252, 107793.	5.1	30
139	Impact of the reproductive organs on crop BRDF as observed from a UAV. Remote Sensing of Environment, 2021, 259, 112433.	11.0	30
140	Gap frequency and canopy architecture of sugar beet and wheat crops. Agricultural and Forest Meteorology, 1993, 65, 261-279.	4.8	29
141	A dynamic model of maize 3D architecture: application to the parameterisation of the clumpiness of the canopy. Agronomy for Sustainable Development, 1998, 18, 609-626.	0.8	29
142	Global Gap-Free MERIS LAI Time Series (2002–2012). Remote Sensing, 2016, 8, 69.	4.0	28
143	Special Issue on Clobal Land Product Validation. IEEE Transactions on Geoscience and Remote Sensing, 2006, 44, 1695-1697.	6.3	27
144	A method to estimate plant density and plant spacing heterogeneity: application to wheat crops. Plant Methods, 2017, 13, 38.	4.3	27

#	Article	IF	CITATIONS
145	Mapping short-wave albedo of agricultural surfaces using airborne PolDER data. Remote Sensing of Environment, 2002, 80, 36-46.	11.0	25
146	Estimation of maize canopy properties from remote sensing by inversion of 1-D and 4-D models. Precision Agriculture, 2010, 11, 319-334.	6.0	25
147	Characterizing reflectance anisotropy of background soil in open-canopy plantations using UAV-based multiangular images. ISPRS Journal of Photogrammetry and Remote Sensing, 2021, 177, 263-278.	11.1	23
148	Atmospheric corrections of single broadband channel and multidirectional airborne thermal infrared data: Application to the ReSeDA experiment. International Journal of Remote Sensing, 2003, 24, 3269-3290.	2.9	21
149	Importance of the description of light interception in crop growth models. Plant Physiology, 2021, 186, 977-997.	4.8	21
150	Crop specific algorithms trained over ground measurements provide the best performance for GAI and fAPAR estimates from Landsat-8 observations. Remote Sensing of Environment, 2021, 260, 112453.	11.0	21
151	Radiative transfer sensitivity to the accuracy of canopy structure description. The case of a maize canopy. Agronomy for Sustainable Development, 1999, 19, 241-254.	0.8	21
152	Modeling temporal changes in surface spatial heterogeneity over an agricultural site. Remote Sensing of Environment, 2008, 112, 588-602.	11.0	20
153	Bridging the Gap Between Remote Sensing and Plant Phenotyping—Challenges and Opportunities for the Next Generation of Sustainable Agriculture. Frontiers in Plant Science, 2021, 12, 749374.	3.6	20
154	Root biomass fraction as a function of growth degree days in wheat. Plant and Soil, 1992, 140, 137-144.	3.7	18
155	Using Thermal Time and Pixel Purity for Enhancing Biophysical Variable Time Series: An Interproduct Comparison. IEEE Transactions on Geoscience and Remote Sensing, 2013, 51, 2119-2127.	6.3	17
156	Combining hectometric and decametric satellite observations to provide near real time decametric FAPAR product. Remote Sensing of Environment, 2017, 200, 250-262.	11.0	17
157	Monitoring Forest Phenology and Leaf Area Index with the Autonomous, Low-Cost Transmittance Sensor PASTiS-57. Remote Sensing, 2018, 10, 1032.	4.0	17
158	Critical analysis of methods to estimate the fraction of absorbed or intercepted photosynthetically active radiation from ground measurements: Application to rice crops. Agricultural and Forest Meteorology, 2021, 297, 108273.	4.8	17
159	Geometrical modelling of soil bidirectional reflectance incorporating specular effects. International Journal of Remote Sensing, 1996, 17, 3691-3704.	2.9	15
160	FASPECT: A model of leaf optical properties accounting for the differences between upper and lower faces. Remote Sensing of Environment, 2021, 253, 112205.	11.0	15
161	Suivi de la maturation de couverts de blé par radiométrie dans les domaines visible et proche infra-rouge. Agronomy for Sustainable Development, 1986, 6, 509-516.	0.8	14
162	Scoring Cercospora Leaf Spot on Sugar Beet: Comparison of UGV and UAV Phenotyping Systems. Plant Phenomics, 2020, 2020, 9452123.	5.9	14

#	Article	IF	CITATIONS
163	SAILHFlood: A radiative transfer model for flooded vegetation. Ecological Modelling, 2013, 257, 25-35.	2.5	13
164	Crop specific inversion of PROSAIL to retrieve green area index (GAI) from several decametric satellites using a Bayesian framework. Remote Sensing of Environment, 2022, 278, 113085.	11.0	13
165	2D approximation of realistic 3D vineyard row canopy representation for light interception (fIPAR) and light intensity distribution on leaves (LIDIL). European Journal of Agronomy, 2011, 35, 171-183.	4.1	12
166	Reply to Townsend et al.: Decoupling contributions from canopy structure and leaf optics is critical for remote sensing leaf biochemistry. Proceedings of the National Academy of Sciences of the United States of America, 2013, 110, E1075.	7.1	12
167	GEOV2/VGT: near real time estimation of global biophysical variables from VEGETATION-P data. , 2013, , .		11
168	Reply to Ollinger et al.: Remote sensing of leaf nitrogen and emergent ecosystem properties. Proceedings of the National Academy of Sciences of the United States of America, 2013, 110, E2438.	7.1	11
169	OPERATIONAL 333m BIOPHYSICAL PRODUCTS OF THE COPERNICUS GLOBAL LAND SERVICE FOR AGRICULTURE MONITORING. International Archives of the Photogrammetry, Remote Sensing and Spatial Information Sciences - ISPRS Archives, 0, XL-7/W3, 53-56.	0.2	11
170	Exploring Seasonal and Circadian Rhythms in Structural Traits of Field Maize from LiDAR Time Series. Plant Phenomics, 2021, 2021, 9895241.	5.9	10
171	Temperature and emissivity extracted from airborne multi-channel data in the ReSeDA experiment. Agronomy for Sustainable Development, 2002, 22, 567-573.	0.8	10
172	Modeling Canopy Spectral Properties to Retrieve Biophysical and Biochemical Characteristics. , 1994, , 145-167.		9
173	PROSPECT+SAIL: 15 Years of Use for Land Surface Characterization. , 2006, , .		9
174	SPOT-VEGETATION GEOV1 biophysical parameters in semi-arid agro-ecosystems. International Journal of Remote Sensing, 2014, 35, 2534-2547.	2.9	9
175	Deforestation in Michoacan, Mexico, From CYCLOPES-LAI Time Series (2000–2006). IEEE Journal of Selected Topics in Applied Earth Observations and Remote Sensing, 2016, 9, 5398-5405.	4.9	9
176	Photosynthetically Active Radiation: Measurement and Modeling. , 2013, , 140-169.		9
177	Genomic Prediction of Green Fraction Dynamics in Soybean Using Unmanned Aerial Vehicles Observations. Frontiers in Plant Science, 2022, 13, 828864.	3.6	9
178	Effective GAI is best estimated from reflectance observations as compared to GAI and LAI: Demonstration for wheat and maize crops based on 3D radiative transfer simulations. Field Crops Research, 2022, 283, 108538.	5.1	9
179	A method for aerosol correction from the spectral variation in the visible and near infrared: application to the MERIS sensor. International Journal of Remote Sensing, 2007, 28, 761-779.	2.9	8
180	Modeling the spatial distribution of plants on the row for wheat crops: Consequences on the green fraction at the canopy level. Computers and Electronics in Agriculture, 2017, 136, 147-156.	7.7	8

#	Article	IF	CITATIONS
181	Comparison of Metrics for the Classification of Soils Under Variable Geometrical Conditions Using Hyperspectral Data. IEEE Geoscience and Remote Sensing Letters, 2008, 5, 755-759.	3.1	7
182	Forest species mapping using airborne hyperspectral APEX data. , 2016, 20, 28-33.		7
183	Development and assessment of leaf area index algorithms for the Sentinel-2 multispectral imager. , 2014, , .		6
184	Evaluation of kernel-driven BRDF models for the normalization of Alpilles/ReSeDA POLDER data. Agronomy for Sustainable Development, 2002, 22, 531-536.	0.8	6
185	Estimating Biophysical Variables at 250 M with Reconstructed EOS/MODIS Time Series to Monitor Fragmented Landscapes. , 2008, , .		5
186	Estimation of Biophysical Variables from Satellite Observations. , 2016, , 37-80.		5
187	Assessment of Three Methods for Near Real-Time Estimation of Leaf Area Index From AVHRR Data. IEEE Transactions on Geoscience and Remote Sensing, 2017, 55, 1489-1497.	6.3	5
188	Using Automatic Differentiation to Study the Sensitivity of a Crop Model. Lecture Notes in Computational Science and Engineering, 2012, , 59-69.	0.3	5
189	Breeding for Economically and Environmentally Sustainable Wheat Varieties: An Integrated Approach from Genomics to Selection. Biology, 2022, 11, 149.	2.8	5
190	Multi-sensor data fusion for deriving bio-physical variables in the cyclopes project. , 0, , .		4
191	CYCLOPES algorithmic development for estimating biophysical products from large swath sensors. , 0, , .		4
192	A multistage database of field measurements and synoptic remotely sensed data to support model validation and testing in Earth observation. Computers and Geosciences, 2011, 37, 1511-1514.	4.2	4
193	Speeding up 3D radiative transfer simulations: A physically based metamodel of canopy reflectance dependency on wavelength, leaf biochemical composition and soil reflectance. Remote Sensing of Environment, 2020, 237, 111614.	11.0	4
194	Analyse des comportements spectraux dans l'olivette de Sfax (Tunisie). Agronomy for Sustainable Development, 1986, 6, 941-948.	0.8	4
195	Improving the Consistency and Continuity of MODIS 8 Day Leaf Area Index Products. International Journal of Electronics and Telecommunications, 2012, 58, 141-146.	0.5	4
196	ESTIMACIÓN DEL ÃNDICE DE ÃREA FOLIAR EN LA RESERVA DE LA BIÓSFERA MARIPOSA MONARCA. Revista Fitotecnia Mexicana, 2010, 33, 169.	0.1	4
197	A method for MERIS atmospheric correction based on the spectral and spatial observation. , 0, , .		3
198	Green Leaf Area and Fraction of Photosynthetically Active Radiation Absorbed by Vegetation. Springer Remote Sensing/photogrammetry, 2014, , 43-61.	0.4	3

#	Article	IF	CITATIONS
199	Characterizing the spatial and temporal variability of biophysical variables of a wheat crop using hyper-spectral measurements. , 0, , .		2
200	Assessing the vertical distribution of leaf chlorophyll content in a maize crop. , 0, , .		2
201	Validation of MSG vegetation products: part I. Field retrieval of LAI and FVC from hemispherical photographs. , 2004, , .		2
202	Modeling forest canopies with a hierarchical multi-ring Boolean model for estimating a leaf area index. Spatial Statistics, 2013, 5, 42-56.	1.9	2
203	Caracterización de la fenologÃa de la vegetación a escala global mediante series temporales SPOT VEGETATION. Revista De Teledeteccion, 2016, , 1.	0.6	2
204	CAPACITY OF PHENOLOGICAL DATA DERIVED FROM CYCLOPES LAI FOR THE YEAR 2000 TO DISTINGUISH LAND COVER TYPES IN THE STATE OF MICHOACÃN, MEXICO. Revista Chapingo, Serie Ciencias Forestales Y Del Ambiente, 2014, XX, 261-276.	0.2	2
205	The Use of Hyperspectral Imagery for Digital Soil Mapping in Mediterranean Areas. , 2010, , 93-102.		2
206	A Double Swath Configuration for Improving Throughput and Accuracy of Trait Estimate from UAV Images. Plant Phenomics, 2021, 2021, 9892647.	5.9	2
207	Use of remote sensing data for nitrogen management in precision farming. , 0, , .		1
208	Understanding vegetation response to climate variability from space: the scientific objectives, the approach and the concept of the SPECTRA mission. , 0, , .		1
209	Evaluation of SPOT/HRV data over temporal series acquired during the ADAM project. , 0, , .		1
210	Assimilating high temporal frequency SPOT data to describe canopy functioning: the ADAM project. , 0, , .		1
211	Understanding vegetation response to climate variability from space: recent advances towards the SPECTRA Mission. , 2004, , .		1
212	Optimization of image parameters using a hyperspectral library application to soil identification and moisture estimation. , 2009, , .		1
213	Optimal band selection for future satellite sensor dedicated to soil science. , 2009, , .		1
214	Monitoring crop growth inter-annual variability from MODIS time series: Performance comparison between crop specific green area index and current global leaf area index products. , 2011, , .		1
215	Production of the high resolution maps of biophysical variables based on SPOT imagery and in-situ measurements generated by PASTIS 57 for Hyytiala, Finland. , 2012, , .		1
216	Near-real time estimates of leaf area index from AVHRR time series data. , 2012, , .		1

#	Article	IF	CITATIONS
217	Validation of MODIS albedo products with high resolution albedo estimates from FORMOSAT-2. , 2013, , .		1
218	Near-surface remote sensing observations for monitoring deciduous broadleaf forest species phenology. , 2014, , .		1
219	Temporal Techniques in Remote Sensing of Global Vegetation. Remote Sensing and Digital Image Processing, 2016, , 217-232.	0.7	1
220	CONSISTENCIA ENTRE LOS MAPAS GLOBALES Y LOS MAPAS REGIONALES DE LA CUBIERTA TERRESTRE EN EL ESTADO DE MICHOACAN, MÉXICO. Revista Chapingo, Serie Ciencias Forestales Y Del Ambiente, 2011, XVII, 343-360.	0.2	1
221	Retrieval of vegetation properties from combined hyperspectral/multiangular optical measurements: results from the DAISEX campaigns. , 0, , .		0
222	CLAMP: accounting for leaf clumping in radiative transfer modelling. , 0, , .		0
223	Model inversion procedure for retrieving wheat biophysical variables from hyperspectral measurements. , 0, , .		0
224	Satellite derived leaf area index derived from SOPT time series in the ADAM project. , 0, , .		0
225	Towards accounting for leaf clumping within radiative transfer modeling. , 0, , .		0
226	How do current GORT models describe the bidirectional reflectance distribution function of forests?. , 0, , .		0
227	Monitoring Evapotranspiration over the Alpilles Test Site by Introducing Remote Sensing Data at Various Spatial Resolutions into a Dynamic SVAT Model. AIP Conference Proceedings, 2006, , .	0.4	0
228	Comparison of metrics to remove the influence of geometrical conditions on soil reflectance. , 2007, ,		0
229	Reflectance modeling of vineyards under water stress based on the coupling between 3D architecture and water balance model. Proceedings of SPIE, 2009, , .	0.8	0
230	The effective nature of LAI as measured from remote sensing observations. , 2010, , .		0
231	Quantification of LAI interannual anomalies by adjusting climatological patterns. , 2011, , .		0
232	A multiscale and multisensor approach of LAI retrieval in a maritime pine ecosystem. , 2012, , .		0
233	Correction to "Using thermal time and pixel purity for enhancing biophysical variable time series: An interproduct comparison" [Apr 13 2119-2127]. IEEE Transactions on Geoscience and Remote Sensing, 2013, 51, 4911-4911.	6.3	0
234	Operational delivery of long time series of biophysical variables in the copernicus land service. , 2013, ,		0

#	Article	IF	CITATIONS
235	Applying remote sensing expertise to crop improvement: progress and challenges to scale up high throughput field phenotyping from research to industry. , 2016, , .		0
236	Reaching Stage 4 of Vegetation Product Validation by Exploiting the Synergy Between UAV, HR Satellites and IoT Measurements. , 2021, , .		0
237	REMOTE SENSING OF ORCHARDS: INFLUENCE OF CANOPY ARCHITECTURE AND OBSERVATIONAL CONDITIONS ON UNCERTAINTIES ASSOCIATED TO KEY CANOPY CHARACTERISTICS ESTIMATES BASED ON 3D MODELS. Acta Horticulturae, 2011, , 19-26.	0.2	0